PLOS Biology

METHODS AND RESOURCES

A broad-host-range *Rhizobium rhizogenes* strain enables transient expression across diverse crop species

Freddie King[1☯], **Juan Carlos Lopez-Agudelo**[2,3,4☯], **Christopher Stephens**[5], **May Htet Aung**[2], **Tarhan Ibrahim**[1], **Enoch Lok Him Yuen**[1], **Ao Chen**[1], **Nick Eilmann**[1], **Saskia Jenkins**[1], **Cristina Vuolo**[1], **Yueh-Ning Swee**[2], **Wei-Jia Liu**[2], **Samuel Bruty**[5,6], **AmirAli Toghani**[7], **Chih-Horng Kuo**[2,3,8], **Erh-Min Lai**[2,3,8], **Jiorgos Kourelis**[1], **Lida Derevnina**[5]*, **Chih-Hang Wu**[2,3,8]*, **Tolga Bozkurt**[1]*

1 Department of Life Sciences, Imperial College London, London, United Kingdom, **2** Institute of Plant and Microbial Biology, Academia Sinica, Taipei, Taiwan, **3** Molecular and Biological Agricultural Sciences Program, Taiwan International Graduate Program, National Chung Hsing University and Academia Sinica, Taipei, Taiwan, **4** Graduate Institute of Biotechnology, National Chung Hsing University, Taichung, Taiwan, **5** Crop Science Centre, Department of Plant Science, University of Cambridge, Cambridge, United Kingdom, **6** Department of Biochemistry and Metabolism, John Innes Centre, Norwich, United Kingdom, **7** The Sainsbury Laboratory, University of East Anglia, Norwich, United Kingdom, **8** Biotechnology Center, National Chung Hsing University, Taichung, Taiwan

☯ These authors contributed equally to this work.
* ld645@cam.ac.uk (LD); wuchh@gate.sinica.edu.tw (C-HW); o.bozkurt@imperial.ac.uk (TB)

Check for updates

OPEN ACCESS

Citation: King F, Lopez-Agudelo JC, Stephens C, Aung MH, Ibrahim T, Yuen ELH, et al. (2026) A broad-host-range *Rhizobium rhizogenes* strain enables transient expression across diverse crop species. PLoS Biol 24(10): e3004010. https://doi.org/10.1371/journal.pbio.3004010

Academic Editor: Xinnian Dong, Duke University, UNITED STATES OF AMERICA

Received: May 7, 2026

Accepted: September 8, 2026

Published: October 15, 2026

Peer Review History: PLOS recognizes the benefits of transparency in the peer review process; therefore, we enable the publication of all of the content of peer review and author responses alongside final, published articles. The editorial history of this article is available here: https://doi.org/10.1371/journal.pbio.3004010

Copyright: © 2026 King et al. This is an open access article distributed under the terms of the Creative Commons Attribution License, which permits unrestricted use, distribution,

Abstract

Agrobacterium-mediated transient expression has revolutionised plant research, enabling numerous landmark discoveries across diverse areas of plant biology. Yet this powerful approach remains largely confined to solanaceous species, leaving most economically important crop families without a comparable rapid assay platform. Here, we show that an engineered *Rhizobium rhizogenes* strain, AS109, mediates efficient transient expression across diverse dicot species spanning multiple taxonomic families, consistently outperforming commonly used laboratory agrobacterial strains. Leveraging the broad host range of AS109, we establish a suite of functional assays in faba bean (*Vicia faba*), including protein localisation, RNA interference-mediated gene silencing, cell-surface elicitor recognition screens, nucleotide-binding leucine-rich repeat receptor (NLR) activation, and infection cell biology at the host-pathogen interface. We further demonstrate that both singleton NLRs and sensor-helper NLR pairs from Solanaceae retain effector recognition and cell death activity when transferred into faba bean, establishing a rapid platform for evaluating cross-family transferability of disease-resistance genes. AS109 thus provides an accessible and versatile chassis for functional genomics in non-model crops, bridging the widening gap between hypothesis generation and experimental validation across diverse plant species.

and reproduction in any medium, provided the original author and source are credited.

Data availability statement: Constructs generated for this study and the strains used will be made available upon request to the Imperial College Research Office Contracts Team (email: g.wheeler@imperial.ac.uk), or the Academia Sinica Department of Intellectual Property and Technology Transfer (via the designated online portal at https://iptt.sinica.edu.tw/pages/4960) and will be subject to completion of a material transfer agreement (MTA). The raw data and scripts underlying each figure have been deposited on Zenodo at https://doi.org/10.5281/zenodo.20056567 [43].

Funding: This work was funded by the following sources: Biotechnology and Biological Sciences Research Council (BBSRC) BB/X016382/1 (T.O.B.) Website: https://www.ukri.org/councils/bbsrc/. Bezos Earth Fund through the Bezos Centre for Sustainable Protein BCSP/IC/001 (T.O.B.) Website: https://www.bezosearthfund.org. Academia Sinica Grand Challenge Program AS-GC-111-L02 (E.M.L., C.H.K. and C.H.W.) Website: https://sub.daais.sinica.edu.tw/grants/gcp_en.html. Intramural fund of the Institute of Plant and Microbial Biology, Academia Sinica (E.M.L., C.H.K. and C.H.W.) Website: https://ipmb.sinica.edu.tw/en. The Niab Trust, through an independent fellowship (L.D.) Website: https://www.niab.com/about-us/people/niab-boards/niab-trust. Royal Society University Research Fellowship URF\R1\251226 (J.K.) Website: https://royalsociety.org/grants/university-research/. European Research Council (ERC) Starting Grant 101220795 – PREDESIGNX (J.K.) Website: https://erc.europa.eu/apply-grant/starting-grant. The funders did not play any role in study design, data collection, analysis, decision to publish or preparation of the manuscript.

Competing interests: I have read the journal's policy and the authors of this manuscript have the following competing interests: T.O.B. receives funding from industry and co-founded a start-up company (Resurrect Bio Ltd.) on NLR biology. L.D. and J.K. have filed patents on NLR biology. L.D. has received funds from Resurrect Bio Ltd. C.H.W. has signed an agreement for future funding from an industrial partner at the time of submission.

Abbreviations: CP, coat protein; dpi, days post-inoculation; EV, empty vector; PRRs, pattern recognition receptors.

Introduction

Advances in genomics and computational biology, including protein structure prediction and large-scale genomic analyses, are rapidly accelerating hypothesis generation in the plant sciences. Yet the capacity to experimentally test these hypotheses has not kept pace, as biological assays remain slow, labour-intensive, and often restricted to a handful of model species. *Agrobacterium*-mediated transient expression, particularly in *Nicotiana benthamiana*, has been a major solution to this experimental bottleneck, enabling rapid experimental validation and landmark discoveries in plant-pathogen interactions, effector biology, immune receptor discovery and function, structural biology, and gene silencing pathways such as RNA interference (RNAi) and virus-induced gene silencing [1–3]. These achievements underscore the transformative power of transient assays for functional studies in plants. However, transient expression remains largely confined to solanaceous species [4], leaving many economically important crop groups, including legumes, brassicas, and Asteraceae without a comparable experimental platform.

Recent efforts to enhance *Agrobacterium*-mediated transient expression have focussed on rewiring virulence gene regulation, optimising plasmid architecture, suppressing host immunity, and refining infiltration conditions [5–8]. While these strategies improve expression levels, a fundamental limitation persists: most transient expression assays rely on *Agrobacterium fabrum* (formerly *A. tumefaciens*) C58-derived strains, whose narrow host range excludes the majority of crop species. We recently developed *Rhizobium rhizogenes* strain AS109 (formerly *Agrobacterium rhizogenes*, referred to as AS109 hereafter) as a new platform for transient expression in solanaceous crops [9]. AS109 was previously developed by disarming *R. rhizogenes* strain A4, which was found to mediate the strongest transient expression in *N. benthamiana* from a panel of 47 diverse agrobacterial strains. Given its distinct genetic background and delivery properties, we asked whether AS109 might support transient expression beyond solanaceous hosts. Here, we show that AS109 exhibits a broad host range spanning diverse dicot families. Given the global importance of legume crops for dietary protein, and the limited transient systems in this family, we sought to use AS109-mediated expression to establish a new model species in Fabaceae. To this end, we use AS109 to build a transient expression system in faba bean (*Vicia faba*), enabling protein localisation, gene silencing, immune receptor assays and infection cell biology. Together, these findings position AS109 as a versatile transient-expression chassis for non-solanaceous crops and provide a practical framework for rapid functional testing of candidate genes and pathways emerging from genomic and computational discovery.

Results

Rhizobium rhizogenes AS109 enables transient expression across diverse dicot crops

To assess the applicability of AS109 across diverse plant species, we compared AS109 with several commonly used laboratory *Agrobacterium* strains (EHA105,

LBA4404, GV3101::pMP90, AGL-1, and C58C1::pTiB6S3ΔT) in 30 plant species representing multiple taxonomic groups and families (Figs 1 and S1–S4; S1 Table). We introduced bacterial suspensions into leaves by simple syringe infiltration, and assessed transient expression efficiency using the RUBY reporter, which encodes three enzymes that convert tyrosine into red-purple betalain pigments, enabling direct visual observation and quantitative analysis [10]. We first focussed on species belonging to Solanaceae, in which AS109 was previously shown to be effective [9]. Consistent with our previous report, AS109 showed superior transient expression efficiency compared with other tested laboratory strains on petunia (*Petunia hybrida*), tobacco (*N. tabacum*), potato (*Solanum tuberosum*), black nightshade (*Solanum nigrum*), goji berry (*Lycium barbarum*), and goldenberry (*Physalis peruviana*) (Figs 1C and S1C). Although *N. tabacum* is widely used for transient expression assays, transformation efficiency can vary substantially between leaves. Notably, while all other tested laboratory strains exhibit poor transient expression in older (lower) leaves, AS109 mediated highly reliable transient expression across different leaves of *N. tabacum* (S2 Fig), consistent with the notion that AS109 is less sensitive to leaf physiological age [9]. This robustness is particularly important for assays with inherently variable readouts, such as immune receptor activation and pathogen infection, where minimising leaf-to-leaf variation across biological and technical replicates is critical for reliable quantification.

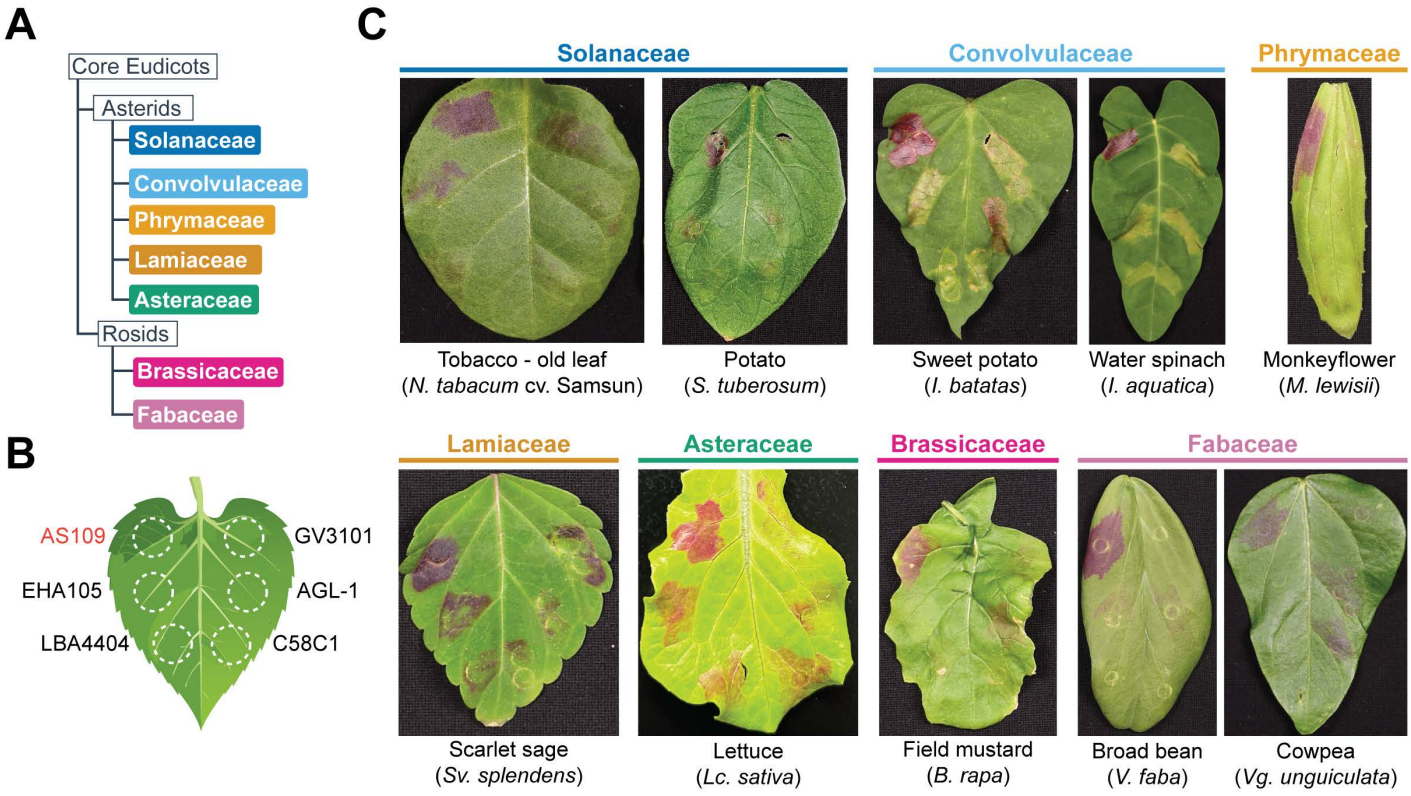


Fig 1. *Rhizobium rhizogenes* AS109 enables transient gene expression across diverse dicot species. (A) Simplified phylogenetic tree showing the evolutionary relationships of the plant families tested for RUBY transient expression. **(B)** Schematic representation of the infiltration layout used to compare six different agrobacterial strains. AS109 is positioned at the top left (highlighted in red). **(C)** Representative photographs of leaves showing transient expression of the RUBY reporter. Results display successful AS109-mediated expression across seven plant families: Solanaceae, Convolvulaceae, Phrymaceae, Lamiaceae, Asteraceae, Brassicaceae, and Fabaceae. All species tested and betalain quantification is shown in S1–S4 Figs. The data underlying this figure can be found at https://doi.org/10.5281/zenodo.20056567.

https://doi.org/10.1371/journal.pbio.3004010.g001

We next examined the applicability of AS109 to several *Ipomoea* species in the family Convolvulaceae. While none of the other tested strains mediated clear and consistent transient reporter expression, AS109 enabled efficient transient expression in young expanding leaves of sweet potato (*I. batatas*), water spinach (*I. aquatica*), and *I. hederacea*, but not in *I. alba* (Figs 1C and S1D). Notably, AS109 induced fewer necrotic symptoms compared with other strains in *Ipomoea* spp., which may partly explain its higher efficiency in these species. This prompted us to extend our analysis to other asterid families and as well as to Caryophyllales (S3A and S3B Fig). AS109 mediated efficient transient expression in leaves of monkey flower (*Mimulus lewisii*; Phrymaceae), scarlet sage (*Salvia splendens*; Lamiaceae), sesame (*Sesamum indicum*; Pedaliaceae), and lettuce (*Lactuca sativa*; Asteraceae) (Figs 1C, S3C, and S3D). In contrast, the other tested laboratory strains exhibited markedly lower expression efficiency in scarlet sage and lettuce, and showed little to no RUBY expression in monkey flower and sesame (Figs 1C, S3C, and S3D). However, none of the tested laboratory strains, including AS109, mediated clear expression in snapdragon (*Antirrhinum majus*; Plantaginaceae), coffee (*Coffea canephora*; Rubiaceae), or red quinoa (*Chenopodium formosanum*; Amaranthaceae) (S3E Fig).

Next, we explored the potential application of AS109 in species from the Brassicaceae and Fabaceae, two rosid plant families that include many economically important crops (Figs 1A, and S4A and S4B). Although AGL-1 and GV3101 mediated weak transient expression in field mustard (*Brassica rapa*; Brassicaceae), AS109 consistently produced stronger transient expression across different leaves (Figs 1C and S4C). We then tested eight species from the Fabaceae family. AS109 mediated consistent transient expression in alfalfa (*Medicago sativa*), fenugreek (*Trigonella foenum-graecum*), snow pea (*Pisum sativum*), common bean (*Phaseolus vulgaris*), faba bean (*Vicia faba*) and cowpea (*Vigna unguiculata*), but not soybean (*Glycine max*) or mung bean (*Vigna radiata*) (Figs 1C and S4D). In contrast, the other tested laboratory strains mediated low or inconsistent transient expression across these species (S4D Fig). Although AS109 did not support transient expression in every species tested, these results demonstrate that AS109 outperforms commonly used laboratory *Agrobacterium* strains in the majority of tested plants, underscoring its broad utility for transient expression across diverse plant taxa.

AS109 facilitates functional assays in the non-model species faba bean and lettuce

To further explore whether AS109 can enable functional study of non-model species, we tested important transient assays in faba bean, owing to its amenability to transient expression in our initial screen and the global importance of Fabaceae crop species (Fig 1C) [11]. Using the RUBY reporter, we verified that AS109 enables stronger transient expression in the first (most apical) and second leaf of faba bean compared to *A. fabrum* GV3101 and C58C1 (Fig 2A and 2B). To test whether AS109 facilitates cell biology study in faba bean, we examined GFP localisation in the leaf epidermal cells by agroinfiltration of GV3101 and AS109 (Fig 2C–2E). Confocal microscopy revealed that AS109-mediated transient expression leads to stronger, more consistent GFP signals across a greater proportion of faba bean epidermal cells. Importantly, AS109-mediated transient expression led to clear GFP signal in key subcellular compartments, the nucleus and cytoplasm (Fig 2C). In addition to overexpression assays, we tested whether AS109-mediated expression could transiently knockdown genes in faba bean by RNAi, using previously established hairpin RNA constructs [12]. To test RNAi in faba bean using AS109, we co-expressed GFP and mCherry fluorescent markers with hairpin GFP and GUS constructs (Fig 2F and 2G). Co-expression with the hairpin GFP construct led to a significant reduction in GFP fluorescence compared to the hairpin GUS control but had no significant effect on fluorescence from the mCherry control. We verified successful RNAi of GFP by RT-PCR, which showed a loss of GFP mRNA in leaves co-expressing hairpin GFP, but not with hairpin GUS (Fig 2H). These results demonstrate that AS109 enables key transient assays in the non-model plant faba bean, facilitating the study of protein localisation and genetics in an important Fabaceae crop species.

To evaluate the generalisability of AS109-mediated transient assays, we performed the same assays in another non-model species, lettuce, a major leafy vegetable crop in the highly diverse Asteraceae family. Consistent with the results above, AS109 facilitated stronger transient expression in lettuce leaves than three commonly used *A. fabrum* strains

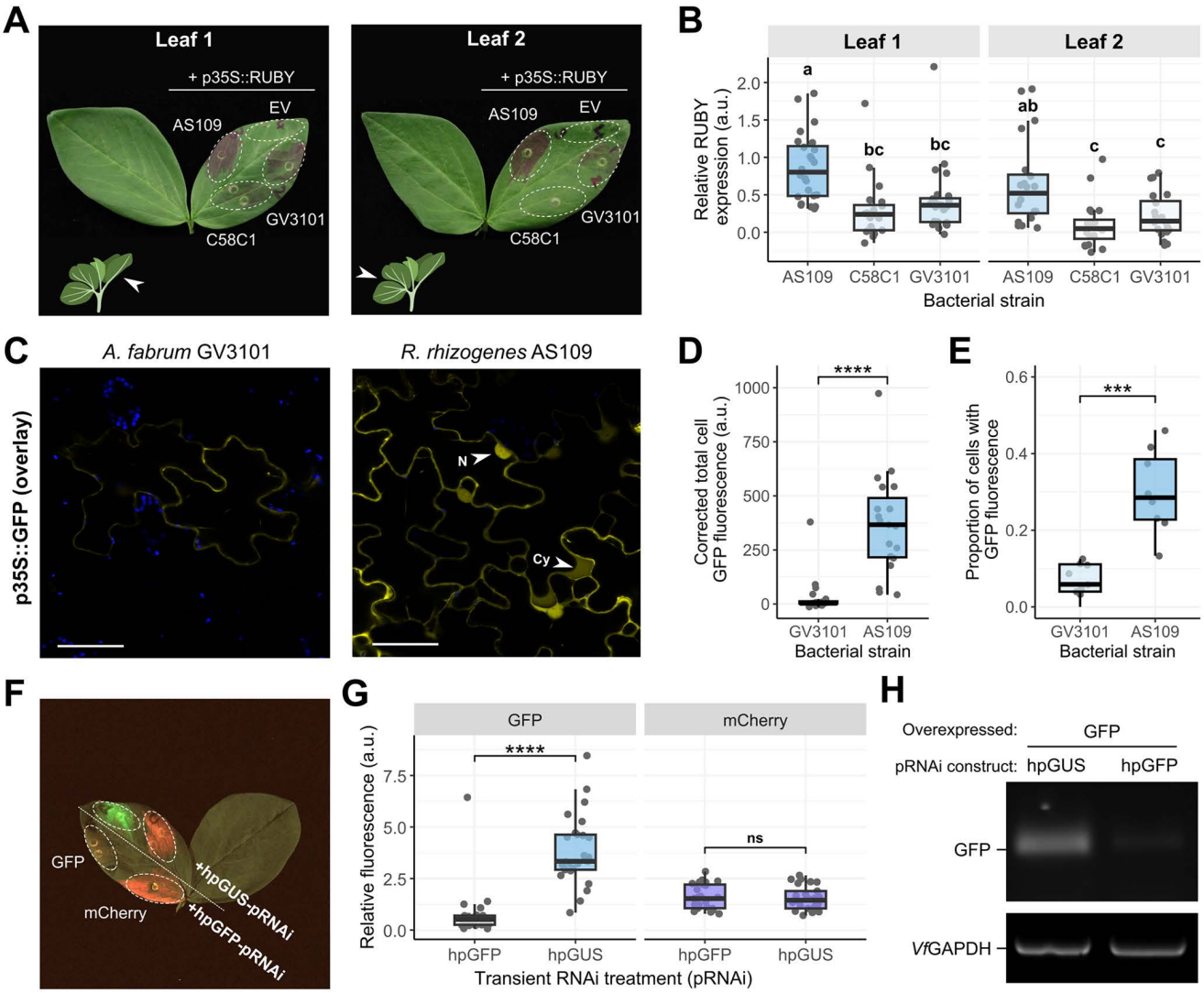


Fig 2. AS109 facilitates functional assays in the non-model species faba bean. (A) A representative image of the first and second faba bean leaf expressing RUBY by agroinfiltration of *A. fabrum* GV3101::pMP90, C58C1::pTiB6S3ΔT or *R. rhizogenes* AS109 compared to an empty vector (EV) control. **(B)** Box and dot plot depicting quantified betalain accumulation, normalised to the EV control, across three agroinfiltrations ($n = 28$). Different letters above box plots represent statistically significant differences between treatments ($p < 0.05$, one-way ANOVA with *post-hoc* Tukey HSD). **(C)** Representative confocal micrographs of faba bean epidermal cells expressing p35S::GFP by agroinfiltration of *A. fabrum* GV3101 or *R. rhizogenes* AS109. White arrows indicate GFP signal in the nucleus (N) and cytoplasm (Cy). Chloroplasts were visualised by autofluorescence at 648–709 nm emission. Scale bars represent 50 μm and both micrographs are single-plane images. **(D)** Box and dot plot depicting corrected total cell GFP fluorescence from faba bean epidermal cells expressing p35S::GFP by infiltration of *A. fabrum* GV3101 or *R. rhizogenes* AS109 ($n = 20$ cells). Asterisks above box plots represent statistically significant differences between treatments ($p < 0.05$, Student *t* test). **(E)** Box and dot plot showing the proportion of cells with GFP fluorescence per field of view of faba bean epidermal cells expressing p35S::GFP ($n = 8$ images). **(F)** Representative stacked fluorescence image of an agroinfiltrated faba bean leaf at 532, 602 and 700 nm emission to visualise GFP fluorescence, mCherry fluorescence, and brightfield, respectively. Fluorescent markers were co-agroinfiltrated with pRNAi hairpin constructs to mediate transient RNAi. **(G)** A box and dot plot depicting quantified GFP and mCherry fluorescence, normalised to background leaf fluorescence, at 532 and 602 nm emission, respectively. Agroinfiltrations were performed three times ($n = 25$). **(H)** Validation of transient knockdown of GFP expression in faba bean by RT-PCR. RT-PCR was performed on cDNA generated from the total RNA of four infiltrated leaves. Glyceraldehyde 3-phosphate dehydrogenase (GAPDH) gene expression served as an internal control. The data underlying this figure can be found at https://doi.org/10.5281/zenodo.20056567.

https://doi.org/10.1371/journal.pbio.3004010.g002

(Figs 1C, S5A, and S5B). To check whether AS109 can enable cell biology studies in lettuce leaves, we compared GFP expression and localisation by agroinfiltration with AS109 and C58C1 (S5C and S5D Fig). Confocal microscopy demonstrated that AS109 caused stronger GFP expression in the epidermal cells than C58C1, evidenced by significantly higher total cell GFP fluorescence, and allows clearer visualisation of the nuclear compartment. To test AS109-mediated RNAi, we co-expressed GFP with hairpin GFP and GUS constructs in lettuce leaves (S5E and S5F Fig). Quantification of GFP fluorescence revealed a significant reduction upon co-expression with hairpin GFP but not hairpin GUS, suggesting that AS109 also allows transient gene knockdown in lettuce. RT-PCR of GFP mRNA also showed a reduction in GFP expression with hairpin GFP (S5G Fig). Taken together, AS109 also facilitates important transient assays in lettuce, extending the possibility of functional assays in multiple non-model crop species.

AS109 enables rapid testing of immune receptors and elicitors in faba bean

Conventional *Agrobacterium*-mediated transient expression in *N. benthamiana* has made major contributions to the functional analysis of plant disease-resistance proteins, particularly nucleotide-binding leucine-rich repeat receptors (NLRs) and cell-surface pattern recognition receptors (PRRs), by enabling rapid tests of receptor autoactivity, signalling requirements, and effector recognition [3]. To evaluate the use of AS109-mediated transient expression for studying immunity in non-model species, we tested the function of autoactive NLRs in faba bean leaves. AS109-mediated transient expression of autoactive solanaceous helper NLRs such as NRC2, NRC3, and NRC4 variants carrying mutations in the MHD motif, but not their WT variants, triggered cell death indicating that NRC helpers can recapitulate their autoactive functions in Fabaceae (Fig 3A and 3B) [13]. As a control for HR, we also expressed a CC-NLR cloned from faba bean (*Vf*CC-NLR) which has a canonical domain structure and is a member of the RPM1-like CC-NLR clade (S6 Fig) [14]. Consistently, expression of autoactive, but not WT, *Vf*CC-NLR triggered cell death. Expression of autoactive NRC4 with additional L to E mutations in the CC domain (*Nb*NRC4$^{DV/3E}$) did not cause HR, showing that NRC4 auto-activity in faba bean requires an intact CC domain, consistent with the earlier results obtained using *N. benthamiana* (Fig 3C and 3D) [15]. To confirm the activation of heterologously expressed NRCs in faba bean, we examined the subcellular distribution of *Nb*NRC4 in its resting and active state. We co-expressed the WT and autoactive, non-cell-death-inducing NRC4 L9E mutant (*Nb*NRC4$^{DV/L9E}$) with the *S. tuberosum* REMORIN marker (*St*REM1.3) in faba bean leaves. *St*REM1.3 is a plasma membrane marker which has been used to monitor helper NLR puncta at the cell surface in *N. benthamiana* [16–18]. Consistent with previous studies, the resting, inactive NRC4 showed a diffuse cytoplasmic distribution but, upon activation, formed membrane-associated puncta (Fig 3E) [16,17]. These results reveal that Solanaceous NRCs can form puncta and trigger cell death in faba bean leaves.

Solanaceae NLRs are relatively well studied compared with those from most other plant families and represent a potential source of novel disease-resistance genes for non-solanaceous crops [19]. However, divergence in required signalling pathways can render many transferred NLRs non-functional, a phenomenon known as restricted taxonomic functionality [20,21]. To assess whether AS109-mediated transient expression enables rapid evaluation of NLR transferability, and to distinguish NLRs that require additional components from those that do not, we performed proof-of-concept experiments by expressing two solanaceous NLRs together with their corresponding avirulence factors in faba bean leaves.

We first tested the cell death function of the singleton NLR Rpi-vnt1 in faba bean leaves (Fig 4A and 4B). Rpi-vnt1 was originally cloned from *Solanum venturii* and provides resistance to *Phytophthora infestans* by recognition of the effector Avr-vnt1 [22]. Transient expression of Rpi-vnt1 under its native promoter in faba bean led to cell death upon co-expression with its cognate effector Avr-vnt1, showing that effector recognition of this singleton NLR can be directly transferred from Solanaceae to Fabaceae without additional components.

Next, we tested the cell death function of the sensor NLR Rx, which recognises the PVX coat protein (CP) and requires NRC helper NLRs to trigger cell death (Fig 4C and 4D) [13,23]. Transient expression of Rx with CP in faba bean triggered cell death only when *Nb*NRC4 was co-expressed, showing that the cell death specificity of sensor NLRs can also

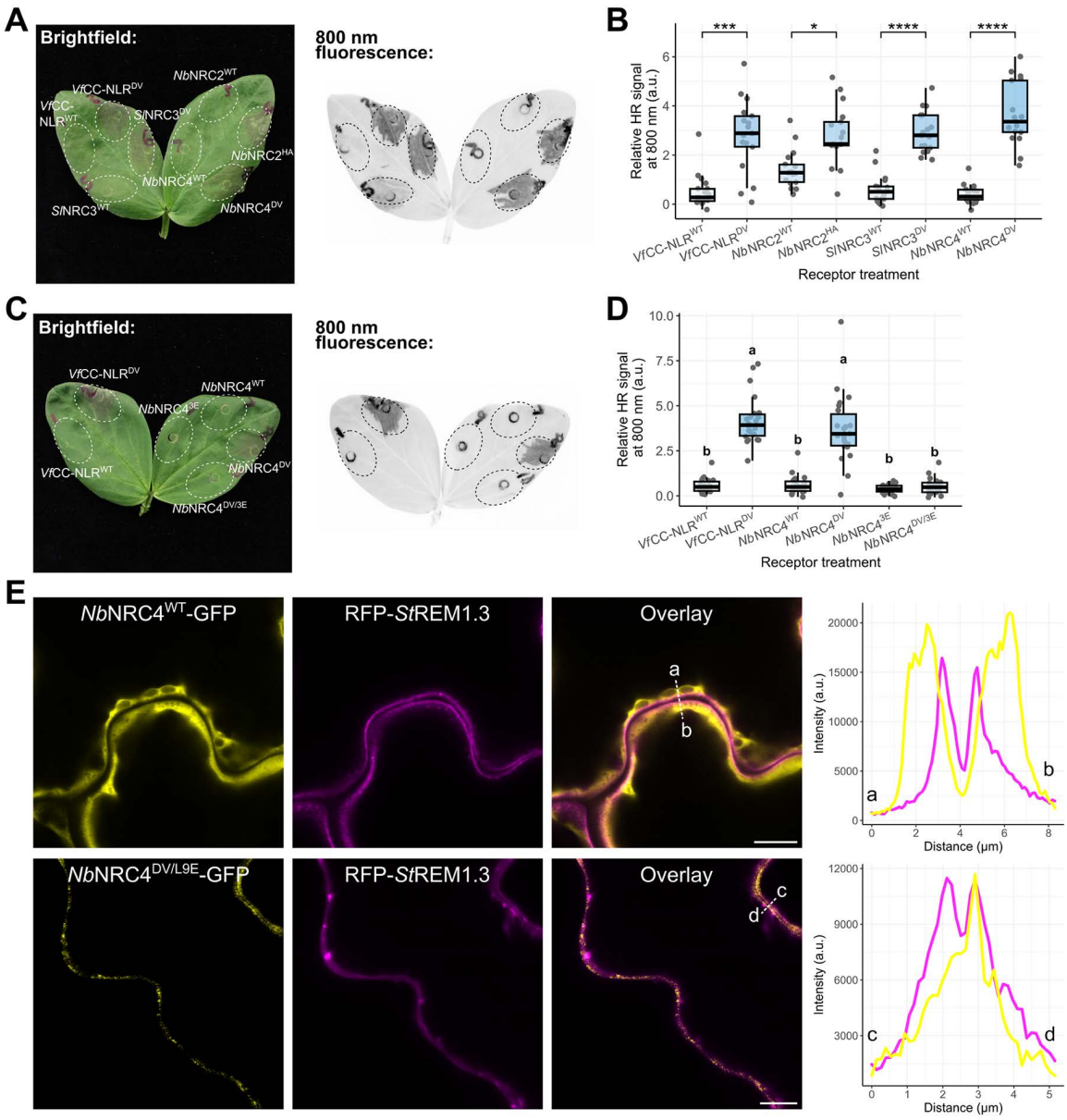


Fig 3. Autoactive helper NLRs cause cell death and form puncta at the plasma membrane in faba bean. (A) Representative image of a faba bean leaf showing HR from expressing WT and autoactive helper NLRs under brightfield (left) and under 800 nm emission (right). Expression of the WT and autoactive variant of a faba bean NLR (*Vf*CC-NLR) served as a negative and positive control, respectively. Expressed NLRs were made autoactive by mutations in the conserved MHD motif (D to V or H to A), and autoactive *Nb*NRC4 was inactivated by additional L to E mutations in the CC domain. **(B)** Box and dot plot showing the quantified HR signal from expressing WT and autoactive helper NLRs at 800 nm emission from infiltrated faba bean leaves, normalised to the background leaf signal. Asterisks above box plots represent statistically significant differences between treatments ($p < 0.05$, Student *t* test with Bonferroni correction). Agroinfiltrations were performed three times ($n = 17$). **(C)** Representative image of a faba bean leaf showing HR from expressing *Nb*NRC4 mutants. Expression of the WT and autoactive variant of a faba bean NLR (*Vf*CC-NLR) served as a negative and positive control, respectively. **(D)** Box and dot plot showing the quantified HR signal of expressing *Nb*NRC4 mutants under 800 nm emission from infiltrated faba bean leaves, normalised to the background leaf signal. Different letters above box plots represent statistically significant differences between treatments ($p < 0.05$, one-way ANOVA with *post-hoc* Tukey HSD). Agroinfiltrations were performed three times ($n = 22$). **(E)** Representative confocal micrographs of faba bean epidermal cells transiently expressing *Nb*NRC4^{WT}-GFP ($n = 5$ images) or *Nb*NRC4$^{DV/L9E}$-GFP ($n = 11$ images) with RFP-*St*REM1.3. *Nb*NRC4 was made autoactive by the D to V mutation, combined with the L9E mutation in the CC domain to prevent cell death. Under resting conditions, *Nb*NRC4 has a cytoplasmic distribution (a,b) but upon activation forms puncta which localise to the plasma membrane **(c,d)**. Transects correspond to the line intensity plots of relative fluorescence intensity across the marked distances. Scale bars represent 10 μm. The data underlying this figure can be found at https://doi.org/10.5281/zenodo.20056567.

https://doi.org/10.1371/journal.pbio.3004010.g003

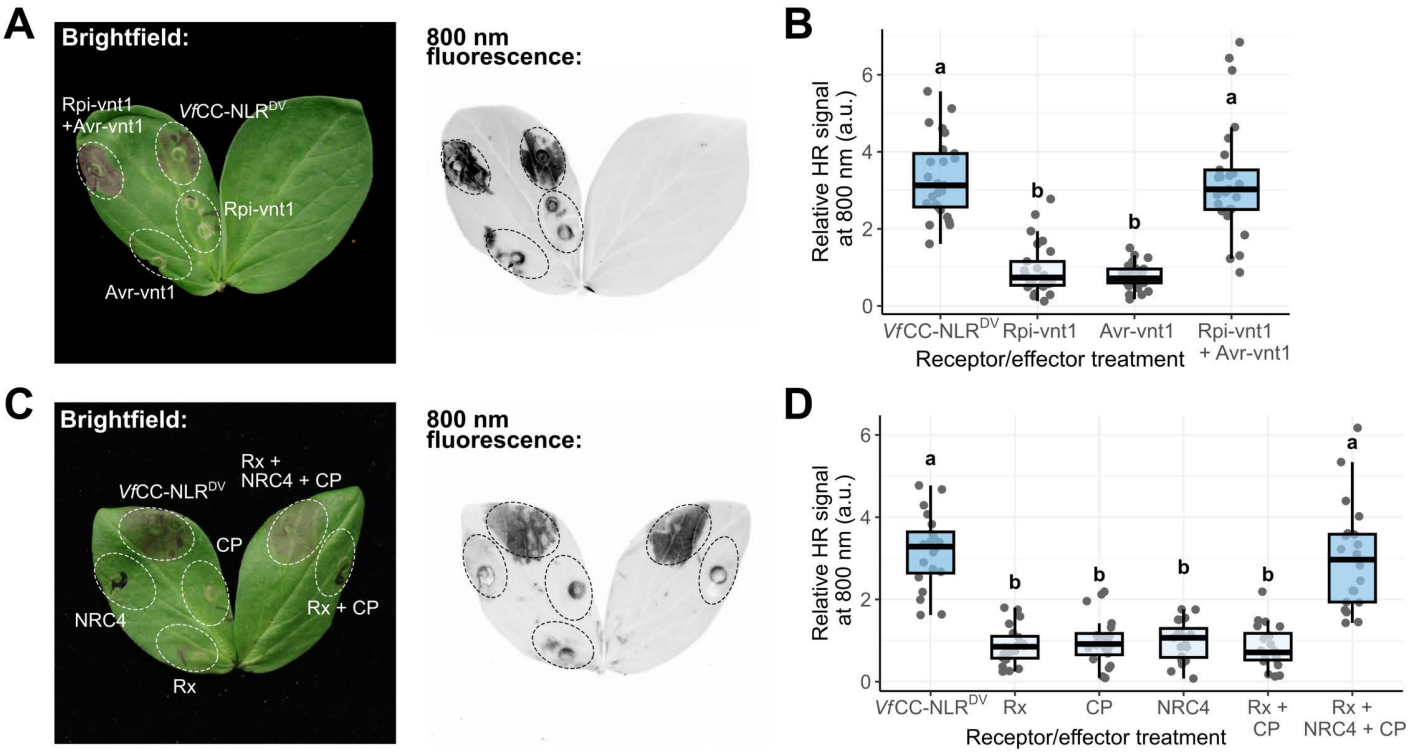


Fig 4. A singleton NLR and a sensor-helper NLR pair from Solanaceae perform their cell death functions in faba bean. (A) Representative image of a faba bean leaf showing HR from expressing combinations of Rpi-vnt1 and Avr-vnt1 under brightfield (left) and under 800 nm emission (right). Expression of an autoactive faba bean NLR (*Vf*CC-NLR^{DV}) served as a positive control. **(B)** Box and dot plot showing the quantified HR under 800 nm emission from infiltrated faba bean leaves, normalised to the background leaf signal. Different letters above box plots represent statistically significant differences between treatments ($p < 0.05$, one-way ANOVA with *post-hoc* Tukey HSD). Agroinfiltrations were performed three times ($n = 25$). **(C)** A representative image of a faba bean leaf under brightfield and under 800 nm emission, showing HR from expressing combinations of Rx, CP and *Nb*NRC4. Expression of an autoactive faba bean NLR (*Vf*CC-NLR^{DV}) served as a positive control. **(D)** Box and dot plot showing the quantified HR signal at 800 nm emission from infiltrated faba bean leaves, normalised to the background leaf signal. Agroinfiltrations were performed three times ($n = 20$). The data underlying this figure can be found at https://doi.org/10.5281/zenodo.20056567.

https://doi.org/10.1371/journal.pbio.3004010.g004

be transferred by providing the required helper NLR. Together, these results demonstrate that both singleton NLRs and sensor-helper NLR pairs from solanaceous plants can be moved into faba bean to provide their native effector recognition and cell death functions. This establishes Solanaceae as a potential source for novel disease-resistance genes for other plant families and highlights AS109 as a rapid platform for testing restricted taxonomic functionality across divergent plant families.

We then tested whether AS109 can be used to assess cell-surface recognition of apoplastic pathogen elicitors and effectors in faba bean. We screened a panel of 23 secreted proteins from oomycete, fungal, bacterial, and nematode plant pathogens, which are required for pathogen virulence and have been reported to trigger immune responses in *N. benthamiana* (S7 Fig and S2 Table). Transient expression of these elicitors triggered varying degrees of cell death in faba bean leaves, including strong cell death caused by the cytotoxic protein *Zt*NLP (S7C Fig) [24]. Remarkably, the conserved effector XEG1 from *Phytophthora sojae* triggered weak cell death in faba bean, suggesting that this species may harbour an unknown PRR that recognises XEG1 (S7D Fig) [25]. These data show that AS109 also enables testing of cell-surface recognition in faba bean, making this a powerful platform to screen for novel sources of disease resistance in legumes.

AS109-mediated expression reveals a novel host–pathogen interface in faba bean

Finally, we asked whether AS109-mediated transient expression in faba bean could support infection cell biology assays, an application that has been particularly powerful in *N. benthamiana* for revealing novel defence and immune-suppression mechanisms at the host-pathogen interface [26]. To test this, we transiently expressed the *St*REM1.3 marker fused to RFP in faba bean leaves and subsequently infected detached leaves with a transgenic *Phytophthora palmivora* line expressing ER-targeted YFP (Fig 5) [27]. In *N. benthamiana* cells, *St*REM1.3 accumulates at the plasma membrane and marks the specialised, host-derived membrane surrounding haustoria (feeding structures) of the oomycete pathogen *P. infestans* [17,18]. Similarly, imaging faba bean cells at 1–2 days post-inoculation revealed clear accumulation of *St*REM1.3 at the plasma membrane and around *P. palmivora* haustoria, marking the extrahaustorial membrane (Fig 5B and 5C) [18]. We

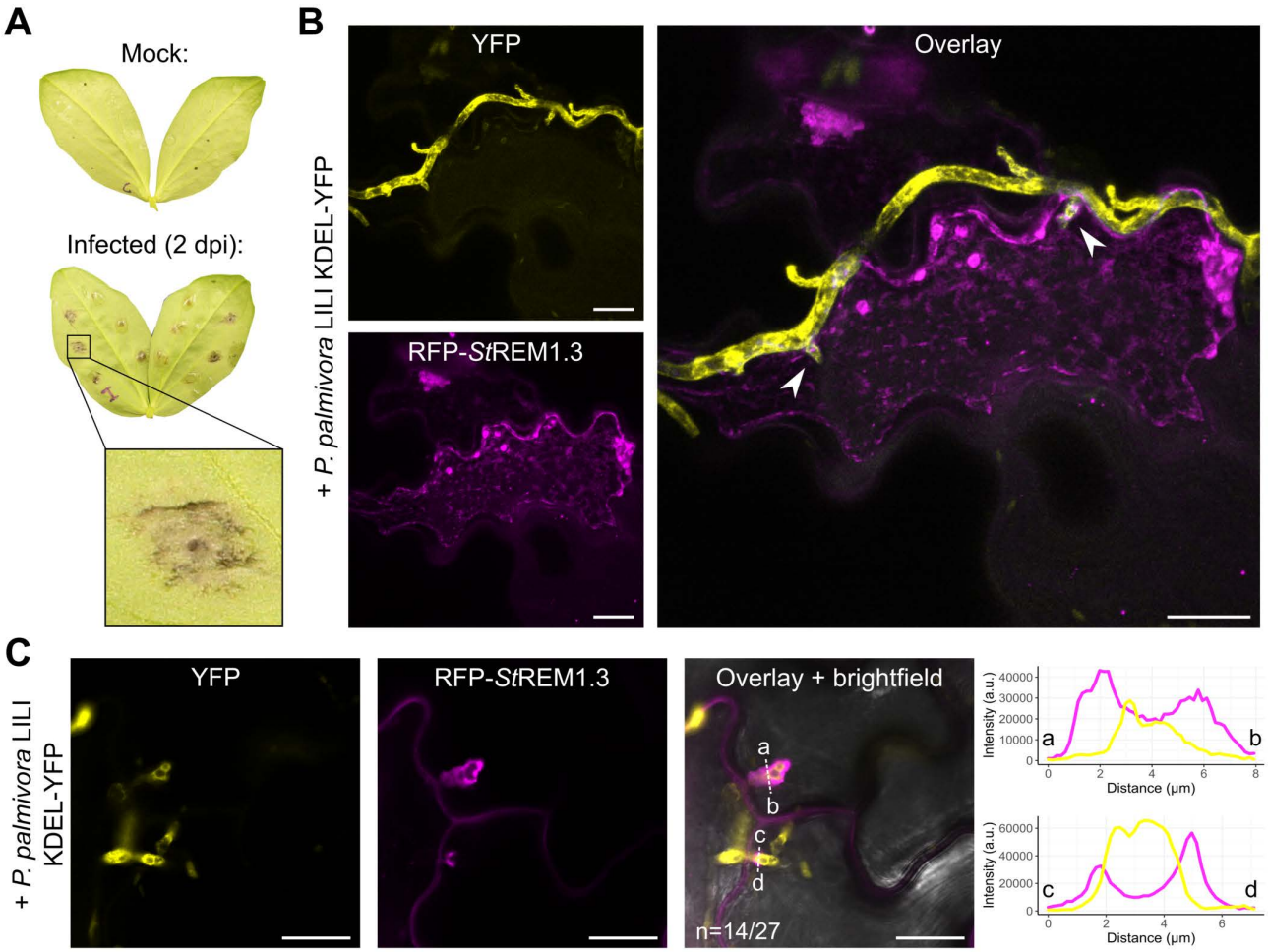


Fig 5. AS109-mediated expression reveals a novel host-pathogen interface in faba bean. (A) Representative image of faba bean leaves mock treated (upper) and infected with *Phytophthora palmivora* LILI KDEL-YFP spores (lower). Photographs were taken at 2 days post-inoculation (dpi). **(B)** Confocal micrograph showing an agroinfiltrated faba bean epidermal cell expressing RFP-*St*REM1.3 whilst infected by *P. palmivora*. The image shown is a maximum projection of z-stacks. Arrows indicate intracellular haustoria. Scale bars represent 20 μm. **(C)** Representative confocal micrographs of faba bean epidermal cells expressing RFP-*St*REM1.3, marking the host-derived extrahaustorial membrane (14/27 haustoria, $n = 10$ images). RFP-*St*REM1.3 both encased entire *P. palmivora* haustoria (a–b) and accumulated specifically at the neck **(c–d)**. Transects correspond to the line intensity plots of relative fluorescence intensity across the marked distances. Scale bars represent 20 μm. The data underlying this figure can be found at https://doi.org/10.5281/zenodo.20056567.

https://doi.org/10.1371/journal.pbio.3004010.g005

observed RFP-*St*REM1.3 both at the neck of *P. palmivora* haustoria and encasing the entire haustoria (Fig 5C). These results show that AS109-mediated transient expression in faba bean is compatible not only with immune receptor assays, but also with infection cell biology approaches for visualising host-pathogen interfaces during infection.

Discussion

In summary, we demonstrate that the *R. rhizogenes* strain AS109 enables robust transient expression across a substantially broader spectrum of wild and crop dicotyledonous species than commonly used laboratory *Agrobacterium* strains. By overcoming long-standing host-range limitations, AS109 provides a versatile and accessible platform for molecular and cell biological analyses in non-model plant species that have remained largely recalcitrant to transient transformation. Its performance across diverse phylogenetic lineages creates new opportunities for comparative studies of plant immunity, signalling, and cell biology in an evolutionary context.

The superior transient expression efficiency and broad host range exhibited by AS109, relative to the other tested agrobacterial strains, suggest that specific genetic determinants underlie these phenotypes. However, identifying these factors remains challenging because AS109 differs extensively from commonly used tumorigenic *Agrobacterium* strains at both chromosomal and plasmid levels. Although the disarmed pRiA4 plasmid represents an obvious candidate, our previous comparison between the pRiA4b-containing strain ARqua1 and the parental A4 strain demonstrated that A4 substantially outperformed ARqua1 for transient expression [9]. These findings indicate that the rhizogenic plasmid alone is insufficient to account for the enhanced transient expression efficiency, suggesting that additional genetic factors are important for AS109-mediated transient expression. Future studies integrating comparative genomics and functional genetics will be required to determine the contributions of the chromosomal background, accessory plasmids, and their interactions, to the transient expression efficiency and expanded host range of AS109.

Beyond basic research, AS109 offers a practical route for rapid gene validation, trait screening, and pathway engineering in crops and wild relatives. In particular, functional interrogation of natural diversity in wild species may accelerate the identification of candidate resistance genes for incorporation into pre-breeding and crop improvement pipelines [28,29]. The success of *Agrobacterium*-mediated transient assays in *N. benthamiana* has helped make Solanaceae a particularly productive system for the discovery and mechanistic analysis of disease-resistance genes, with especially strong progress in R-gene identification and cloning in crops such as potato [30,31]. By extending comparable rapid assays into Fabaceae, AS109 could similarly accelerate the discovery and functional testing of legume disease-resistance traits and mechanisms. As protein structure prediction and comparative genomics continue to accelerate hypothesis generation in plant science, AS109 provides a much-needed platform for rapid functional validation across diverse species, helping to bridge the gap between computational prediction, mechanistic insight, and translational crop improvement.

AS109 also helps overcome redundancy-related challenges in plant immune assays. By enabling immune receptors to be tested across divergent crop families, it offers a tractable heterologous system for dissecting receptor function in genetic backgrounds with reduced endogenous redundancy. This could be especially powerful for resolving helper-sensor NLR relationships, which in native hosts often require complex knockdown or knockout strategies to separate overlapping helper activities [32]. Collectively, our work establishes AS109 as a broadly applicable tool that expands the experimental repertoire of plant biotechnology and accelerates the discovery of novel disease-resistance traits and mechanisms for crop improvement.

Materials and methods

Plant growth conditions

All plant species were grown in climate-controlled growth chambers at 22–28 °C with 16/8 hour day/night light cycles. Most plants were grown on a combination of soil and vermiculite mixed at a 3:1 ratio and were agroinfiltrated at 3–5 weeks old. Faba bean (cultivar ‘de Monica’) and lettuce (cultivar ‘Amica’) plants were grown in Levington’s F2 soil with

sand and Sinclair's 2–5 mm vermiculite, mixed in a 3:1 ratio. Faba bean plants were agroinfiltrated at 1–2 weeks old and lettuce were agroinfiltrated at 2–3 weeks old. The cultivars and origin of all plant material used in this study are detailed in S1 Table.

Molecular cloning

Constructs made in this study were cloned using Golden Gate Modular Cloning (MoClo) with the MoClo Plant Parts [33]. Level 0 gene inserts were produced by commercial gene synthesis (Twist Bioscience) except for *Vf*CC-NLR (gene Vfaba.Hedin2.R1.2g009560.1), which was cloned by PCR from faba bean cDNA (S3 Table) [11]. Constructs were verified by sequencing before transformation into *A. fabrum* strains or *R. rhizogenes* AS109 by electroporation. Construct sequences were designed and verified in Geneious Prime (v2026.0.2). The remaining constructs were provided from previous studies (S4 Table).

Agroinfiltration for transient expression

Agroinfiltration of all plant species was performed as previously described for *Nicotiana benthamiana* [34]. *Agrobacterium* strains containing binary plasmids were grown on 523 or LB plates containing selective antibiotics (100 μg/mL kanamycin or 100 μg/mL spectinomycin) and a secondary antibiotic to maintain the virulence plasmid according to the strain (S5 Table). *R. rhizogenes* AS109 containing binary plasmids was grown on 523 media plates containing selective antibiotics (100 μg/mL kanamycin or 200 μg/mL spectinomycin) and rifampicin (50 μg/mL). For the initial expression comparisons across plant species (Fig 1), all strains were grown on 523 media. Bacterial cells were collected from the plates, washed with distilled water, and resuspended in agroinfiltration buffer (10 mM MES, 10 mM $MgCl_2$, pH 5.7). The OD_{600} of the bacterial suspension was measured using a spectrophotometer and adjusted to the desired OD_{600} according to the requirements of the experiment. The prepared bacterial mixtures were incubated with 150 μM acetosyringone for at least one hour in the dark prior to agroinfiltration. For all plant species, the mixtures were infiltrated into the first (most apical) fully expanded leaf, unless indicated otherwise, using a 1 mL Plastipak syringe without a needle.

RUBY (betalain) quantification

Betalain extraction and quantification were performed as previously described [35]. Briefly, leaf discs from the infiltration spots were collected and incubated in an extraction buffer (10% ethanol, 0.1% formic acid). Betalain was calculated by using a spectrophotometer to obtain the betacyanins (OD_{535}) and betaxanthins (OD_{475}) values, then subtracting the value measured at OD_{600}. For sweet potato, water spinach and common bean, leaf discs were ground in 200 μL of extraction buffer and left under gentle agitation for 10 min. Samples were then centrifuged at 4,000 rpm for 10 min, and 100 μL samples were taken to calculate betalain absorbance.

In faba bean (cultivar 'de Monica'), betalain accumulation following RUBY expression was quantified using image analysis, as previously described [36]. Photographs of agroinfiltrated leaves were taken with a Canon EOS 700D camera under standardised settings. Using ImageJ, images were split into RGB channels and the mean pixel density of the agroinfiltrated area was measured in the green channel. The inverse of the green channel measurement was taken as a proxy for pigment intensity.

Cell death assays

R. rhizogenes AS109 containing the required binary plasmid was agroinfiltrated into the abaxial side of faba bean leaves. At 4 days post-infiltration (dpi), leaves were imaged and cell death was recorded under the IR800 CW (800 nm) channel using the Bio-Rad ChemiDoc MP Imaging System. Signal in the 800 nm channel was quantified using the 'Volume Analysis' tool in Bio-Rad Image Lab software. The 800 nm signal was normalised to the background or EV signal from the same leaf, depending on the experimental design, and plotted using ggplot2 in R version 4.5.2 [37].

Confocal laser scanning microscopy

Confocal microscopy (without infection) was performed on live leaf samples 2–3 dpi. Leaf samples of infiltrated areas were taken using a size 4 cork borer, submerged in distilled water, and mounted on glass slides with glass coverslips. The abaxial side of the leaf discs was imaged using the Leica STELLARIS 1 inverted confocal microscope with a 20× dry or 63× water immersion objective lens. The emission wavelengths for GFP/YFP, BFP and RFP markers were set to 495–550 nm, 402–457 nm and 570–620 nm, respectively. The single-plane confocal micrographs were processed using Leica LAS X software and analysed using ImageJ. To calculate corrected total cell GFP fluorescence, epidermal cells were manually selected to measure integrated density, and neighbouring regions for background fluorescence correction. Corrected total cell GFP fluorescence was calculated for each cell as integrated density minus the area of the cell multiplied by mean fluorescence of the background. To measure the proportion of cells with GFP fluorescence, cells were counted manually using the Multi-point tool.

RNA extraction, cDNA synthesis, and RT-PCR

For RNA extraction, two leaf discs from each of four agroinfiltrated faba bean leaves were taken using a size 4 cork borer. The leaf discs were flash-frozen in liquid nitrogen and total RNA was extracted using the TRIzol RNA Isolation Reagent (Invitrogen) according to the manufacturer's guidelines. Extracted RNA concentration was measured using a NanoDrop Lite Spectrophotometer (Thermo Fisher Scientific) and 2 μg of RNA underwent DNase treatment using RQ1 ribonuclease-free deoxyribonuclease (Promega). The treated RNA was used as a template for cDNA synthesis by Super-Script IV Reverse Transcriptase (Invitrogen) and subsequent PCR reactions were performed using Q5 High-Fidelity DNA Polymerase (New England Biolabs). Expression of the glyceraldehyde-3-phosphate dehydrogenase (GAPDH) housekeeping gene was used as a transcriptional control (faba bean gene Vfaba.Hedin2.R1.4g150200.1; lettuce gene LOC111886224) [11,38]. The RT-PCRs for GFP expression were performed using primers GFP RT-PCR F7 and GFP RT-PCR R2, for faba bean GAPDH using primers VfGAPDH RT-PCR F3 and VfGAPDH RT-PCR R4, and for lettuce GAPDH using primers Ls_GAPDH_qPCR_F3 and Ls_GAPDH_qPCR_R3 (S3 Table).

Phytophthora palmivora growth conditions and infection assays

The transgenic *Phytophthora palmivora* LILI KDEL-YFP strain (accession P16830) has been previously described [27]. *P. palmivora* was cultured on V8 agar plates, supplemented with 100 mg/L G418, at 28 °C for 5–7 days before spore collection. Spores were collected by incubating 15 mL of glass-distilled water on a cultured plate for 45 min at 22 °C. Faba bean leaves were agroinfiltrated 2 days prior to infection. Infections were performed with 10 μL spore droplets on the abaxial side of faba bean leaves and incubated at 22 °C for 24–48 hours before imaging by confocal microscopy.

Phylogenetic analysis

Faba bean NLRs were annotated by running NLRtracker on the predicted proteins of *V. faba* var. Hedin2 [11,39]. The deduplicated NB-ARC domains were aligned with NB-ARC sequences from reference eudicot NLRs in the RefPlantNLR dataset using Clustal Omega version 1.2.4 [39,40]. Amino acid replacement models were assessed by Bayesian information criterion, and the "WAG" model was selected for generating the phylogenetic tree. The maximum likelihood phylogenetic tree was generated with 100 bootstraps using the pharngorn package in R [41]. The tree was visualised with bootstrap values using the ggtree package in R [42].

Data analysis and statistics

All data visualisation and statistics were performed in R, using ggplot2 and tidyverse packages [37]. All scripts used for data analysis and statistics are available on Zenodo [43].

Supporting information

S1 Fig. AS109 mediates successful transient gene expression within the Solanales. (**A**) Detailed phylogeny of the 30 angiosperm species evaluated for RUBY transient expression. The selection spans the Core Eudicots, including Superasterids (Caryophyllales and Asterids) and Rosids. The Solanales lineage (Solanaceae and Convolvulaceae) is highlighted in red. (**B**) Schematic representation of the infiltration layout used to compare six different agrobacterial strains. AS109 is positioned at the top left (highlighted in red). (**C, D**) Representative photographs and betalain quantification for Solanaceae (**C**) and Convolvulaceae (**D**). Photographs display species that were not shown in Fig 1. Box plots represent the total betalain absorbance measurement in each infiltration spot (Solanaceae $n = 12$; *I. batatas* $n = 4$; *I. aquatica* $n = 6$; *I. hederacea* $n = 10$). Different letters above box plots represent statistically significant differences between strains ($p < 0.05$, one-way ANOVA with *post-hoc* Tukey HSD). The data underlying this figure can be found at https://doi.org/10.5281/zenodo.20056567.
(TIF)

S2 Fig. AS109 mediates reliable transient expression across different *N. tabacum* leaves. (**A**) Schematic representation of the infiltration layout used to compare six different agrobacterial strains. AS109 is positioned at the top left (highlighted in red). (**B, C**) Representative photographs and betalain quantification for leaves of different physiological ages in *Nicotiana tabacum* cv. Samsun (**B**) and cv. Xanthi (**C**). Box plots represent the total betalain absorbance measurement in each infiltration spot from leaves 3 (older) through 6 (younger) ($n = 6$). Different letters above box plots represent statistically significant differences between strains ($p < 0.05$, one-way ANOVA with *post-hoc* Tukey HSD). The data underlying this figure can be found at https://doi.org/10.5281/zenodo.20056567.
(TIF)

S3 Fig. AS109 mediates successful transient gene expression across several non-Solanales Superasterid families. (**A**) Detailed phylogeny of the 30 angiosperm species evaluated for RUBY transient expression. The selection spans the Core Eudicots, including Superasterids (Caryophyllales and Asterids) and Rosids. The Superasterids lineages detailed in this figure (Lamiales, Gentianales, Asterales and Caryophyllales) are highlighted in red. (**B**) Schematic representation of the infiltration layout used to compare six different agrobacterial strains. AS109 is positioned at the top left (highlighted in red). (**C**) Box plots representing the total betalain absorbance measurement in each infiltration spot in species with successful RUBY expression (*M. lewisii* $n = 11$; *Sv. splendens* $n = 8$; *Lc. sativa* $n = 13$). Different letters above box plots represent statistically significant differences between strains ($p < 0.05$, one-way ANOVA with *post-hoc* Tukey HSD). (**D, E**) Representative photographs of species exhibiting weak (**D**) or undetectable (**E**) RUBY expression. The data underlying this figure can be found at https://doi.org/10.5281/zenodo.20056567.
(TIF)

S4 Fig. AS109 mediates successful transient gene expression across Brassicaceae and Fabaceae. (**A**) Detailed phylogeny of the 30 angiosperm species evaluated for RUBY transient expression. The selection spans the Core Eudicots, including Superasterids (Caryophyllales and Asterids) and Rosids. The Rosids lineage (Brassicaceae and Fabaceae) is highlighted in red. (**B**) Schematic representation of the infiltration layout used to compare six different agrobacterial strains. AS109 is positioned at the top left (highlighted in red). (**C, D**) Representative photographs and betalain quantification for Brassicaceae (**C**) and Fabaceae (**D**). Photographs display species that were not shown in Fig 1. Box plots represent the total betalain absorbance measurement in each infiltration spot (*B. rapa* $n = 11$; *Me. sativa* $n = 10$; *T. foenum-graecum* $n = 7$; *Pi. sativum*, *V. faba* and *Vg. unguiculata* $n = 12$; *Ps. vulgaris* $n = 10$). Different letters above box plots represent statistically significant differences between strains ($p < 0.05$, one-way ANOVA with *post-hoc* Tukey HSD). The data underlying this figure can be found at https://doi.org/10.5281/zenodo.20056567.
(TIF)

S5 Fig. AS109 facilitates functional assays in the non-model species lettuce. (**A**) Representative image of a lettuce leaf expressing RUBY by agroinfiltration with the indicated *A. fabrum* strains and *R. rhizogenes* AS109. (**B**) Box and dot plot depicting quantified betalain concentration measured by OD_{562} nm across two agroinfiltrations (n = 12). Different letters above box plots represent statistically significant differences between treatments ($p < 0.05$, one-way ANOVA with *post-hoc* Tukey HSD). (**C**) Representative confocal micrographs of lettuce epidermal cells expressing p35S::GFP by agroinfiltration of *A. fabrum* C58C1::pTiB6S3ΔT or *R. rhizogenes* AS109. The white arrow indicates GFP signal in the nucleus (N). Chloroplasts were visualised by autofluorescence at 648–709 nm emission. Scale bars represent 50 μm and both micrographs are single-plane images. (**D**) Box and dot plot depicting corrected total cell GFP fluorescence from lettuce epidermal cells expressing p35S::GFP by infiltration of *A. fabrum* C58C1 or *R. rhizogenes* AS109 ($n = 60$ cells). Agroinfiltrations were repeated three times. Asterisks above box plots represent statistically significant differences between treatments ($p < 0.05$, Student *t* test with Bonferroni correction). (**E**) Representative GFP fluorescence (500–550 nm emission) image of an agroinfiltrated lettuce leaf expressing p35S::GFP with a hairpin GFP RNAi construct or a hairpin GUS control. (**F**) A box and dot plot depicting quantified GFP fluorescence, normalised to background leaf fluorescence at 532 nm emission. Agroinfiltrations were repeated twice ($n = 24$). (**G**) Validation of transient knockdown of GFP expression in lettuce by RT-PCR. RT-PCR was performed on cDNA generated from the total RNA of three infiltrated leaves. Glyceraldehyde 3-phosphate dehydrogenase (GAPDH) gene expression served as an internal control. The data underlying this figure can be found at https://doi.org/10.5281/zenodo.20056567.
(TIF)

S6 Fig. *Vf*CC-NLR is a member of the RPM1-like CC-NLR clade of faba bean NLRs. Maximum-likelihood phylogenetic tree depicting all NLRs annotated from the faba bean (var. Hedin2) genome [11]. Clade labels indicate the NLR class: CC-NLRs with Rx-type CC domains; CC_{G10}-NLRs with G10-type CC domains; CC_R NLRs with RPW8-like CC domains; TIR-NLRs containing a TIR domain. The position of *Vf*CC-NLR is indicated by the red arrow. Characterised eudicot NLRs from RefPlantNLR were used as reference sequences [39], and values represent proportional support of key nodes from 100 bootstraps. The data underlying this figure can be found at https://doi.org/10.5281/zenodo.20056567.
(TIF)

S7 Fig. Apoplastic elicitors trigger cell death in faba bean. (**A–D**) Representative image of a faba bean leaf showing cell death from expressing apoplastic elicitors under 800 nm emission (left) and box-and-dot plot (right) showing the quantified cell death signal, normalised to the background leaf signal, for four groups of elicitors. Expression of the autoactive variant of a faba bean NLR (*Vf*CC-NLR) served as a positive control in each case. Agroinfiltrations were performed twice ($n = 16$). Different letters above box plots represent statistically significant differences between treatments ($p < 0.05$, one-way ANOVA with *post-hoc* Tukey HSD). Details of the apoplastic elicitors can be found in S2 Table. The data underlying this figure can be found at https://doi.org/10.5281/zenodo.20056567.
(TIF)

S1 Table. Plant material used in this study.
(DOCX)

S2 Table. Apoplastic elicitors screened for cell death in faba bean.
(DOCX)

S3 Table. Oligos used for cloning and RT-PCR.
(DOCX)

S4 Table. All constructs used in this study.
(DOCX)

S5 Table. Details of all *Agrobacterium* and *Rhizobium* strains used in this study.
(DOCX)

S1 Raw images. Uncropped blot images used for Figs 2H and S5G.
(PDF)

Acknowledgments

We thank Dr. Chun-Neng Wang (Institute of Ecology and Evolutionary Biology, National Taiwan University) for sharing the seeds of *Mimulus lewisii*, Dr. Heng-Ming Ting (Institute of Plant Biology, National Taiwan University) for sharing the seeds of *V. radiata*, Dr. Na-Sheng Lin (Institute of Plant and Microbial Biology, Academia Sinica) for sharing the seeds of *Chenopodium formosanum*, Dr. Ya-Chun Chang (Department of Plant Pathology and Microbiology, National Taiwan University) for sharing the seeds of *Nicotiana tabacum*.

We thank the Imperial College FILM facility for their technical expertise and provision of our microscopy equipment.

Author contributions

Conceptualization: Freddie King, Juan Carlos Lopez-Agudelo, Christopher Stephens, Lida Derevnina, Chih-Hang Wu, Tolga Bozkurt.

Data curation: Freddie King, Juan Carlos Lopez-Agudelo, Christopher Stephens.

Formal analysis: Freddie King, Juan Carlos Lopez-Agudelo.

Funding acquisition: Chih-Horng Kuo, Erh-Min Lai, Jiorgos Kourelis, Lida Derevnina, Chih-Hang Wu, Tolga Bozkurt.

Investigation: Freddie King, Juan Carlos Lopez-Agudelo, Christopher Stephens, May Htet Aung, Tarhan Ibrahim, Enoch Lok Him Yuen, Ao Chen, Nick Eilmann, Saskia Jenkins, Cristina Vuolo, Yueh-Ning Swee, Wei-Jia Liu.

Methodology: Freddie King, Juan Carlos Lopez-Agudelo, Christopher Stephens, May Htet Aung, Tarhan Ibrahim, Ao Chen, Nick Eilmann, Saskia Jenkins, Cristina Vuolo, Yueh-Ning Swee, Wei-Jia Liu, Samuel Bruty, AmirAli Toghani.

Project administration: Freddie King, Chih-Horng Kuo, Erh-Min Lai, Jiorgos Kourelis, Lida Derevnina, Chih-Hang Wu, Tolga Bozkurt.

Resources: Samuel Bruty, AmirAli Toghani, Chih-Horng Kuo, Erh-Min Lai, Jiorgos Kourelis, Lida Derevnina, Chih-Hang Wu.

Supervision: Freddie King, Juan Carlos Lopez-Agudelo, Chih-Horng Kuo, Erh-Min Lai, Jiorgos Kourelis, Lida Derevnina, Chih-Hang Wu, Tolga Bozkurt.

Validation: Freddie King, May Htet Aung, Tarhan Ibrahim, Enoch Lok Him Yuen.

Visualization: Freddie King, Juan Carlos Lopez-Agudelo, Tarhan Ibrahim, Enoch Lok Him Yuen.

Writing – original draft: Freddie King, Juan Carlos Lopez-Agudelo, Christopher Stephens, Lida Derevnina, Chih-Hang Wu, Tolga Bozkurt.

Writing – review & editing: Freddie King, Juan Carlos Lopez-Agudelo, Christopher Stephens, Chih-Horng Kuo, Erh-Min Lai, Jiorgos Kourelis, Lida Derevnina, Chih-Hang Wu, Tolga Bozkurt.

References

1. Lawson AW, Macha A, Neumann U, Gunkel M, Chai J, Behrmann E, et al. Purifying recombinant proteins from *Nicotiana benthamiana* for structural studies. Nat Protoc. 2026;21(4):1662–81. https://doi.org/10.1038/s41596-025-01249-2 PMID: 40926020
2. Yang Z, Xu W. *Nicotiana benthamiana* as a model system for dissecting plant-pathogen interactions. Front Plant Sci. 2026;17:1770827. https://doi.org/10.3389/fpls.2026.1770827 PMID: 41852564

3. Bally J, Jung H, Mortimer C, Naim F, Philips JG, Hellens R, et al. The rise and rise of *Nicotiana benthamiana*: A plant for all reasons. Annu Rev Phytopathol. 2018;56:405–26. https://doi.org/10.1146/annurev-phyto-080417-050141 PMID: 30149789
4. Wroblewski T, Tomczak A, Michelmore R. Optimization of Agrobacterium-mediated transient assays of gene expression in lettuce, tomato and *Arabidopsis*. Plant Biotechnol J. 2005;3(2):259–73. https://doi.org/10.1111/j.1467-7652.2005.00123.x PMID: 17173625
5. Matsuda R. The impacts of environmental factors and culture conditions on the transient expression of recombinant protein in *Nicotiana benthamiana* under controlled environments. Plant Biotechnol J. 2026;24(1):55–65. https://doi.org/10.1111/pbi.70453 PMID: 41239771
6. Goralogia GS, Willig C, Strauss SH. Engineering Agrobacterium for improved plant transformation. Plant J. 2025;121(5):e70015. https://doi.org/10.1111/tpj.70015 PMID: 40051182
7. Aliu E, Ji Q, Wlazlo A, Grosic S, Azanu MK, Wang K, et al. Enhancing Agrobacterium-mediated plant transformation efficiency through improved ternary vector systems and auxotrophic strains. Front Plant Sci. 2024;15:1429353. https://doi.org/10.3389/fpls.2024.1429353 PMID: 39109064
8. Beritza K, Watts EC, van der Hoorn RAL. Improving transient protein expression in agroinfiltrated *Nicotiana benthamiana*. New Phytol. 2024;243(3):846–50. https://doi.org/10.1111/nph.19894 PMID: 38849321
9. Lopez-Agudelo JC, Goh F-J, Tchabashvili S, Huang Y-S, Huang C-Y, Lee K-T, et al. *Rhizobium rhizogenes* A4-derived strains mediate hyper-efficient transient gene expression in *Nicotiana benthamiana* and other solanaceous plants. Plant Biotechnol J. 2026;24(1):131–44. https://doi.org/10.1111/pbi.70083 PMID: 40203188
10. He Y, Zhang T, Sun H, Zhan H, Zhao Y. A reporter for noninvasively monitoring gene expression and plant transformation. Hortic Res. 2020;7(1):152. https://doi.org/10.1038/s41438-020-00390-1 PMID: 33024566
11. Jayakodi M, Golicz AA, Kreplak J, Fechete LI, Angra D, Bednář P, et al. The giant diploid faba genome unlocks variation in a global protein crop. Nature. 2023;615(7953):652–9. https://doi.org/10.1038/s41586-023-05791-5 PMID: 36890232
12. Yan P, Shen W, Gao X, Li X, Zhou P, Duan J. High-throughput construction of intron-containing hairpin RNA vectors for RNAi in plants. PLoS One. 2012;7(5):e38186. https://doi.org/10.1371/journal.pone.0038186 PMID: 22675447
13. Wu C-H, Abd-El-Haliem A, Bozkurt TO, Belhaj K, Terauchi R, Vossen JH, et al. NLR network mediates immunity to diverse plant pathogens. Proc Natl Acad Sci U S A. 2017;114(30):8113–8. https://doi.org/10.1073/pnas.1702041114 PMID: 28698366
14. Grant MR, Godiard L, Straube E, Ashfield T, Lewald J, Sattler A, et al. Structure of the *Arabidopsis* RPM1 gene enabling dual specificity disease resistance. Science. 1995;269(5225):843–6. https://doi.org/10.1126/science.7638602 PMID: 7638602
15. Adachi H, Contreras MP, Harant A, Wu C-H, Derevnina L, Sakai T, et al. An N-terminal motif in NLR immune receptors is functionally conserved across distantly related plant species. Elife. 2019;8:e49956. https://doi.org/10.7554/eLife.49956 PMID: 31774397
16. Ibrahim T, King FJ, Toghani A, Wang L, Jenkins S, Yuen ELH, et al. A helper NLR channels organellar calcium to trigger plant immunity. Science. 2026;392(6797):499–505. https://doi.org/10.1126/science.aeb6690 PMID: 42060733
17. Duggan C, Moratto E, Savage Z, Hamilton E, Adachi H, Wu C-H, et al. Dynamic localization of a helper NLR at the plant-pathogen interface underpins pathogen recognition. Proc Natl Acad Sci U S A. 2021;118(34):e2104997118. https://doi.org/10.1073/pnas.2104997118 PMID: 34417294
18. Bozkurt TO, Richardson A, Dagdas YF, Mongrand S, Kamoun S, Raffaele S. The Plant membrane-associated REMORIN1.3 accumulates in discrete perihaustorial domains and enhances susceptibility to phytophthora infestans. Plant Physiol. 2014;165(3):1005–18.
19. Oh S, Kim M-S, Kang HJ, Kim T, Kong J, Choi D. Conserved effector families render *Phytophthora* species vulnerable to recognition by NLR receptors in nonhost plants. Nat Commun. 2024;15(1):10070. https://doi.org/10.1038/s41467-024-54452-2 PMID: 39567537
20. Du X, Alam M, Witek K, Milnes L, Houghton J, Lin X, et al. Interfamily co-transfer of sensor and helper NLRs extends immune receptor functionality between angiosperms. Cell. 2025;188(17):4505-4516.e14. https://doi.org/10.1016/j.cell.2025.05.028 PMID: 40532698
21. Guo H, Jones JDG. PRRs and NLRs sans frontières: advances and challenges in transfer of immune receptors between plant species. Curr Opin Biotechnol. 2026;97:103429. https://doi.org/10.1016/j.copbio.2025.103429 PMID: 41520516
22. Foster SJ, Park T-H, Pel M, Brigneti G, Sliwka J, Jagger L, et al. Rpi-vnt1.1, a Tm-2(2) homolog from *Solanum venturii*, confers resistance to potato late blight. Mol Plant Microbe Interact. 2009;22(5):589–600. https://doi.org/10.1094/MPMI-22-5-0589 PMID: 19348576
23. Contreras MP, Pai H, Thompson R, Marchal C, Claeys J, Adachi H, et al. The nucleotide-binding domain of NRC-dependent disease resistance proteins is sufficient to activate downstream helper NLR oligomerization and immune signaling. New Phytol. 2024;243(1):345–61. https://doi.org/10.1111/nph.19818 PMID: 38757730
24. Motteram J, Küfner I, Deller S, Brunner F, Hammond-Kosack KE, Nürnberger T, et al. Molecular characterization and functional analysis of MgNLP, the sole NPP1 domain-containing protein, from the fungal wheat leaf pathogen Mycosphaerella graminicola. Mol Plant Microbe Interact. 2009;22(7):790–9. https://doi.org/10.1094/MPMI-22-7-0790 PMID: 19522561
25. Ma Z, Song T, Zhu L, Ye W, Wang Y, Shao Y, et al. A Phytophthora sojae Glycoside Hydrolase 12 Protein Is a Major Virulence Factor during Soybean Infection and Is Recognized as a PAMP. Plant Cell. 2015;27(7):2057–72. https://doi.org/10.1105/tpc.15.00390 PMID: 26163574
26. Bozkurt TO, Kamoun S. The plant-pathogen haustorial interface at a glance. J Cell Sci. 2020;133(5):jcs237958. https://doi.org/10.1242/jcs.237958 PMID: 32132107
27. Rey T, Chatterjee A, Buttay M, Toulotte J, Schornack S. Medicago truncatula symbiosis mutants affected in the interaction with a biotrophic root pathogen. New Phytol. 2015;206(2):497–500. https://doi.org/10.1111/nph.13233 PMID: 25495186

28. Liu Y, Wang J, Zuo C, Fan W, Yuan C, Zeng J, et al. Identification of a gene conferring broad-spectrum orthotospovirus resistance in Solanaceae. Sci Adv. 2025;11(25):eadw4333. https://doi.org/10.1126/sciadv.adw4333 PMID: 40532009
29. Lin X, Jia Y, Heal R, Prokchorchik M, Sindalovskaya M, Olave-Achury A, et al. Solanum americanum genome-assisted discovery of immune receptors that detect potato late blight pathogen effectors. Nat Genet. 2023;55(9):1579–88. https://doi.org/10.1038/s41588-023-01486-9 PMID: 37640880
30. Jones JDG, Staskawicz BJ, Dangl JL. The plant immune system: From discovery to deployment. Cell. 2024;187(9):2095–116. https://doi.org/10.1016/j.cell.2024.03.045 PMID: 38670067
31. Zhu S, Li Y, Vossen JH, Visser RGF, Jacobsen E. Functional stacking of three resistance genes against Phytophthora infestans in potato. Transgenic Res. 2012;21(1):89–99. https://doi.org/10.1007/s11248-011-9510-1 PMID: 21479829
32. Adachi H, Kamoun S. NLR receptor networks in plants. Essays Biochem. 2022;66(5):541–9. https://doi.org/10.1042/EBC20210075 PMID: 35593644
33. Engler C, Youles M, Gruetzner R, Ehnert T-M, Werner S, Jones JDG, et al. A golden gate modular cloning toolbox for plants. ACS Synth Biol. 2014;3(11):839–43. https://doi.org/10.1021/sb4001504 PMID: 24933124
34. Yuen ELH, Tumtas Y, King F, Ibrahim T, Chan LI, Evangelisti E, et al. A pathogen effector co-opts a host RabGAP protein to remodel pathogen interface and subvert defense-related secretion. Sci Adv. 2024;10(40):eado9516. https://doi.org/10.1126/sciadv.ado9516 PMID: 39365859
35. Chiang B-J, Lin K-Y, Chen Y-F, Huang C-Y, Goh F-J, Huang L-T, et al. Development of a tightly regulated copper-inducible transient gene expression system in *Nicotiana benthamiana* incorporating a suicide exon and Cre recombinase. New Phytol. 2024;244(1):318–31. https://doi.org/10.1111/nph.20021 PMID: 39081031
36. Chen J, Luo M, Hands P, Rolland V, Zhang J, Li Z, et al. A split GAL4 RUBY assay for visual in planta detection of protein-protein interactions. Plant J. 2023;114(6):1209–26. https://doi.org/10.1111/tpj.16234 PMID: 37323061
37. Wickham H, Averick M, Bryan J, Chang W, McGowan L, François R, et al. Welcome to the Tidyverse. JOSS. 2019;4(43):1686. https://doi.org/10.21105/joss.01686
38. Reyes-Chin-Wo S, Wang Z, Yang X, Kozik A, Arikit S, Song C, et al. Genome assembly with in vitro proximity ligation data and whole-genome triplication in lettuce. Nat Commun. 2017;8:14953. https://doi.org/10.1038/ncomms14953 PMID: 28401891
39. Kourelis J, Sakai T, Adachi H, Kamoun S. RefPlantNLR is a comprehensive collection of experimentally validated plant disease resistance proteins from the NLR family. PLoS Biol. 2021;19(10):e3001124. https://doi.org/10.1371/journal.pbio.3001124 PMID: 34669691
40. Sievers F, Wilm A, Dineen D, Gibson TJ, Karplus K, Li W, et al. Fast, scalable generation of high-quality protein multiple sequence alignments using Clustal Omega. Mol Syst Biol. 2011;7:539. https://doi.org/10.1038/msb.2011.75 PMID: 21988835
41. Schliep KP. Phangorn: phylogenetic analysis in R. Bioinformatics. 2011;27(4):592–3.
42. Yu G, Smith DK, Zhu H, Guan Y, Lam TT. ggtree: an r package for visualization and annotation of phylogenetic trees with their covariates and other associated data. Methods Ecol Evol. 2016;8(1):28–36. https://doi.org/10.1111/2041-210x.12628
43. King F, Lopez-Agudelo JC, Stephens C, May Htet A, Ibrahim T, Yuen ELH et al. A broad-host-range *Rhizobium rhizogenes* strain enables transient expression across diverse crops and establishes functional assays in faba bean; 2026 [cited 2026 July 8] Database: Zenodo [Internet] Available from: https://doi.org/10.5281/zenodo.20056567